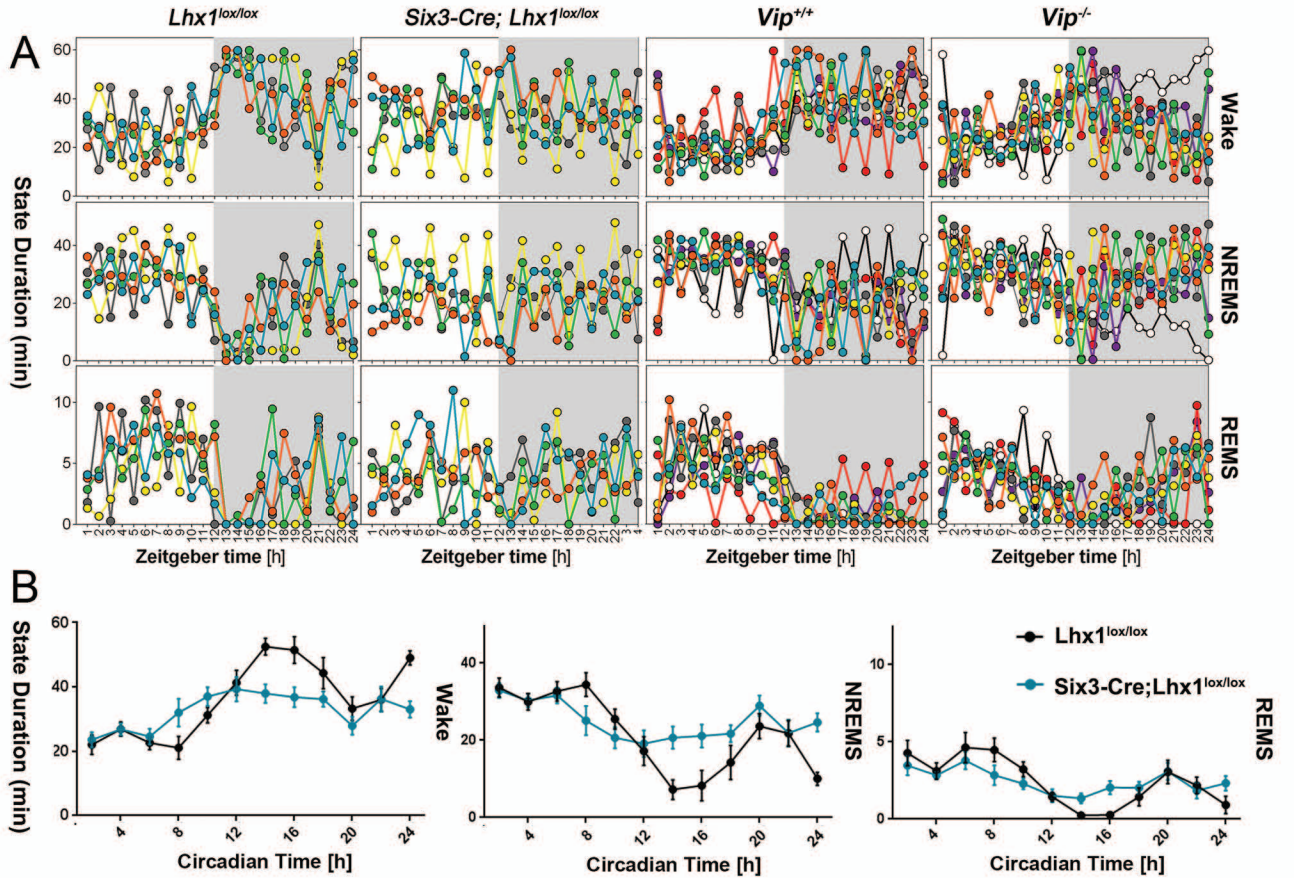
A
Lhx1lox/lox
Six3-Cre; Lhx1lox/lox
Vip+/+
Vip-/-
State Duration (min)
Wake
NREMS
REMS
Zeitgeber time [h]
B
State Duration (min)
Circadian Time [h]
Wake
NREMS
REMS
Lhx1lox/lox
Six3-Cre;Lhx1lox/lox

Figure S1

Figure S1 (Related to Figure 1): Individual LD and Averaged DD Sleep Rhythms in *Six3-Cre;Lhx1$^{lox/lox}$* Mice

(A) Line graphs in which each colored line plots the time spent by a different individual (from left to right) *Lhx1$^{lox/lox}$* control, *Six3-Cre;Lhx1$^{lox/lox}$* mutant, *Vip$^{+/+}$* control, and *Vip$^{-/-}$* mutant mouse in wake (top), NREMS (middle), and REMS (bottom) across a 24-hour cycle in 12:12 LD. Note that individual *Six3-Cre;Lhx1$^{lox/lox}$* mice exhibit frequently fluctuating and sometimes ultradian sleep/wake behavior that is masked in averaged analyses.

(B) Line graphs showing average percent time spent in wake, NREMS, and REMS by *Lhx1$^{lox/lox}$* control (black) and *Six3-Cre;Lhx1$^{lox/lox}$* mutant (blue) mice across a 24-hour cycle in DD. (Graphs show mean +/- SEM.)

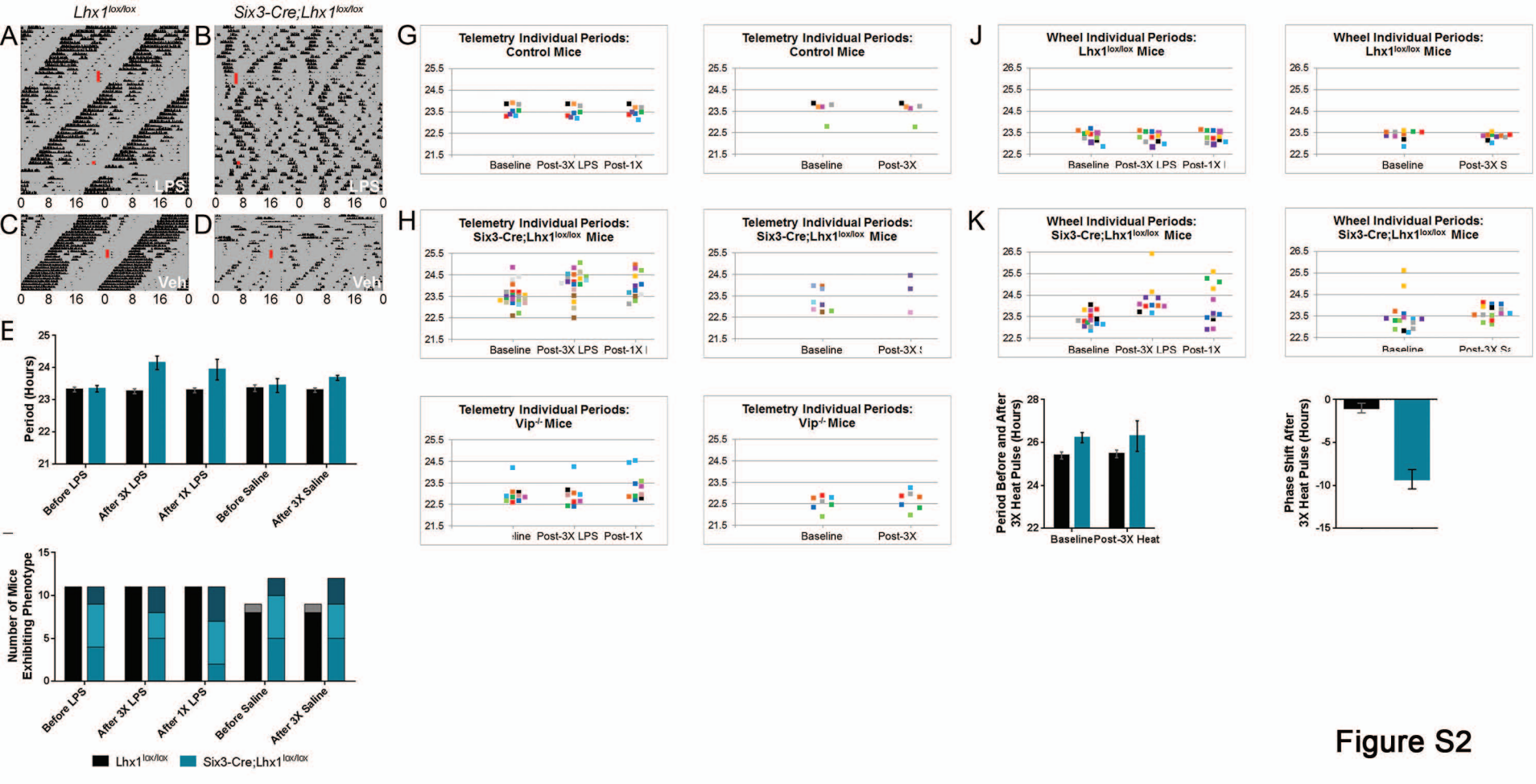
Lhx1lox/lox
Six3-Cre;Lhx1lox/lox
A
B
C
D
LPS
Veh
0 8 16 0 8 16 0
E
Period (Hours)
Before LPS
After 3X LPS
After 1X LPS
Before Saline
After 3X Saline
Number of Mice Exhibiting Phenotype
Lhx1lox/lox
Six3-Cre;Lhx1lox/lox
G
Telemetry Individual Periods: Control Mice
Baseline Post-3X LPS Post-1X
Baseline Post-3X
H
Telemetry Individual Periods: Six3-Cre;Lhx1lox/lox Mice
Telemetry Individual Periods: Vip-/- Mice
J
Wheel Individual Periods: Lhx1lox/lox Mice
K
Wheel Individual Periods: Six3-Cre;Lhx1lox/lox Mice
Period Before and After 3X Heat Pulse (Hours)
Baseline Post-3X Heat
Phase Shift After 3X Heat Pulse (Hours)

Figure S2

Figure S2 (Related to Figure 2): Additional LPS and *Per2::Luc* Data and Analyses
We repeated our LPS study on running wheels to determine whether *Six3-Cre;Lhx1*$^{lox/lox}$ responses generalized across circadian behaviors
(A-B) Sample wheel running actograms from *Lhx1*$^{lox/lox}$ (A) and *Six3-Cre;Lhx1*$^{lox/lox}$ (B) mice in DD. During recording, they received a train of three daily LPS injections (long red rectangle), and later a single LPS injection (red square).
(C-D) Sample wheel running actograms from *Lhx1*$^{lox/lox}$ (C) and *Six3-Cre;Lhx1*$^{lox/lox}$ (D) mice in DD. During recording, they received a train of three daily saline injections (long red rectangle).
(E) 3X LPS elongated average period in *Six3-Cre;Lhx1*$^{lox/lox}$ (blue) mutants; this effect was lost after 1X LPS. *Lhx1*$^{lox/lox}$ (black) mice showed no period response to 3X or 1X LPS. 3X saline was unable to elongate period in *Six3-Cre;Lhx1*$^{lox/lox}$ mutants. Only within-genotype comparisons are shown (Supplemental Data Set; two-way ANOVA with Tukey post-hocs; **p<0.01; graphs show mean +/- SEM; only within-genotype comparisons to baseline are shown).
(F) Neither 3X nor 1X LPS significantly affected the number of rhythms in *Six3-Cre;Lhx1*$^{lox/lox}$ (blue) or *Lhx1*$^{lox/lox}$ (black) mice. 3X saline similarly had no significant effect on this parameter. (Supplemental Data Set; 2x3 Fisher's exact test; only within-genotype comparisons to baseline are shown)
(G-I) Scatter plots showing the period of each individual rhythm from control (G), *Six3-Cre;Lhx1*$^{lox/lox}$ (H), and *Vip*$^{-/-}$ (I) mice in our telemetry study, before and after LPS (left) and saline control (right). Each distinct color indicates rhythm(s) belonging to an individual mouse.
(J-K) Scatter plots showing the period of each individual rhythm from *Lhx1*$^{lox/lox}$ control (J) and *Six3-Cre;Lhx1*$^{lox/lox}$ (K) mice in our wheel-running study, before and after LPS (left) and saline control (right). Each distinct color indicates rhythm(s) belonging to an individual mouse.
(L) Periods of *Per2::Luc* rhythms after 3X heat in *Lhx1*$^{lox/lox}$ and rhythmic-at-baseline *Six3-Cre;Lhx1*$^{lox/lox}$ SCN (n=4,4; Student's t-test; ***p<0.001; mean +/- SEM).
(M) Phase shifts of *Per2::Luc* rhythms after 3X heat in *Lhx1*$^{lox/lox}$ and rhythmic-at-baseline *Six3-Cre;Lhx1*$^{lox/lox}$ SCN (n=4,4; Student's t-test; ***p<0.001; mean +/- SEM).

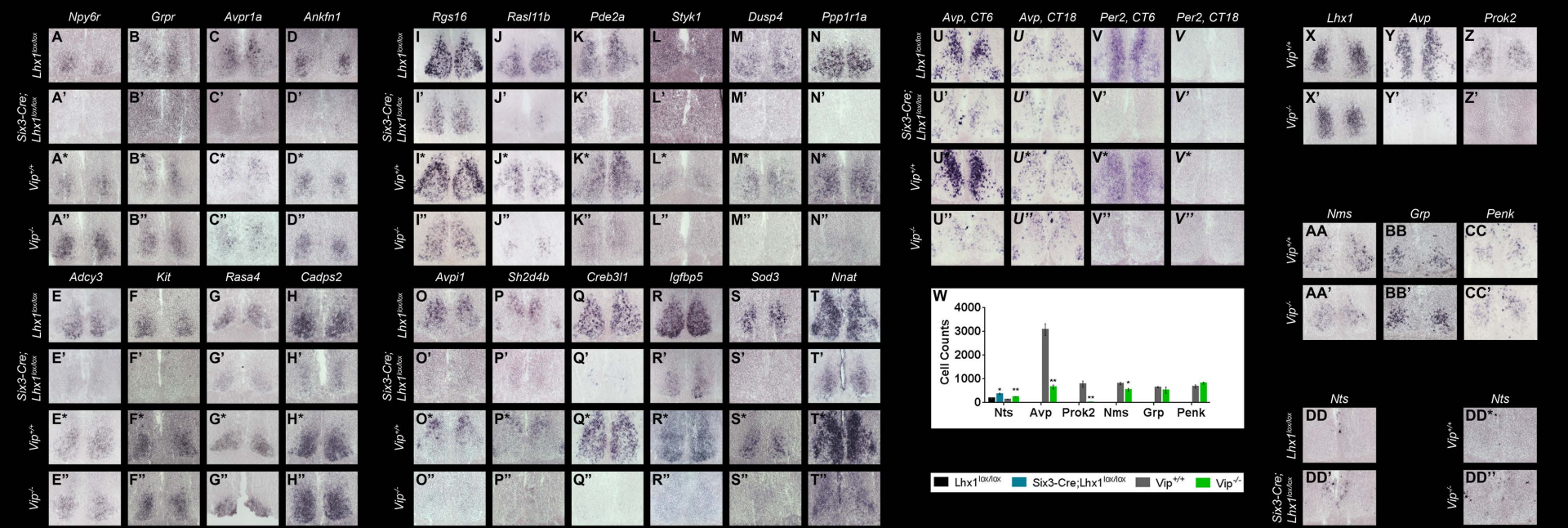
Npy6r
Grpr
Avpr1a
Ankfn1
Rgs16
Rasl11b
Pde2a
Styk1
Dusp4
Ppp1r1a
Avp, CT6
Avp, CT18
Per2, CT6
Per2, CT18
Lhx1
Avp
Prok2
Adcy3
Kit
Rasa4
Cadps2
Avpi1
Sh2d4b
Creb3l1
Igfbp5
Sod3
Nnat
Nms
Grp
Penk
Nts
Nts
Lhx1lox/lox
Six3-Cre; Lhx1lox/lox
Vip+/+
Vip-/-
W
Cell Counts
4000
3000
2000
1000
0
Nts
Avp
Prok2
Nms
Grp
Penk
Lhx1lox/lox
Six3-Cre;Lhx1lox/lox
Vip+/+
Vip-/-

Figure S3

Figure S3 (Related to Figure 4): ISH Analysis of Vip-Dependent and Vip-Independent Effects of Lhx1 on SCN Gene Expression and Core Clock Function

(A-H'') ISH of *Lhx1*$^{lox/lox}$, *Six3-Cre;Lhx1*$^{lox/lox}$, *Vip*$^{+/+}$, and *Vip*$^{-/-}$ SCN for *Npy6r* (A-A''), *Grpr* (B-B''), *Avpr1a* (C-C''), *Ankfn1* (D-D''), *Adcy3* (E-E''), *Kit* (F-F''), *Rasa4* (G-G''), and *Cadps2* (H-H'').

(I-T'') ISH of *Lhx1*$^{lox/lox}$, *Six3-Cre;Lhx1*$^{lox/lox}$, *Vip*$^{+/+}$, and *Vip*$^{-/-}$ SCNs for *Rgs16* (I-I''), *Rasl11b* (J-J''), *Pde2a* (K-K''), *Styk1* (L-L''), *Dusp4* (M-M''), *Ppp1r1a* (N-N''), *Avpi1* (O-O''), *Sh2d4b* (P-P''), *Creb3l1* (Q-Q''), *Igfbp5* (R-R''), *Sod3* (S-S''), and *Nnat* (T-T'').

(U-V'') ISH of SCN from adult *Lhx1*$^{lox/lox}$ control, *Six3-Cre;Lhx1*$^{lox/lox}$ mutant, *Vip*$^{+/+}$ control, and *Vip*$^{-/-}$ mutant mice collected at the peak (CT6, un-italicized letters) and trough (CT18, italicized letters) of the circadian gene expression rhythm for *Avp* (U-U'') and *Per2* (V-V'').

(W) Neuropeptide ISH-labeled SCN cell counts showed more estimated counts per hemisphere for *Nts* cells in both *Six3-Cre;Lhx1*$^{lox/lox}$ and *Vip*$^{-/-}$ mutants; fewer for *Avp*, *Prok2*, and *Nms* cells in *Vip*$^{-/-}$ mutants; and no significant change in *Grp* and *Penk* cells in *Vip*$^{-/-}$ mutants (n=3, paired two-tailed t-tests, *p<0.05; **p<0.01; graph depicts mean +/- SEM). All of these latter neuropeptides have previously been shown to be down in *Six3-Cre;Lhx1*$^{lox/lox}$ SCN.

(X-CC') ISH of adult *Vip*$^{+/+}$ and *Vip*$^{-/-}$ SCN for *Lhx1* (X,X'), *Avp* (Y,Y'), *Prok2* (Z-Z'), *Nms* (AA,AA'), *Grp* (BB,BB'), and *Penk* (CC,CC').

(DD-DD'') ISH for *Nts* in adult *Lhx1*$^{lox/lox}$, *Six3-Cre;Lhx1*$^{lox/lox}$, *Vip*$^{+/+}$, and *Vip*$^{-/-}$ SCN.

Supplemental Data Set (Related to All Figures): Statistical Summaries for All Experiments and ISH Probe List

All statistics for our sleep, LPS, and gene expression studies are included in this Excel spreadsheet. Also included is a list of how all probes used for our ISH studies were obtained or generated.

Supplemental Experimental Procedures:

Supplemental Sleep Analysis
For ultradian analysis, time spent in wake, NREMS, and REMS was segregated into 15-minute bins. This data was plotted in Excel to estimate the approximate period of the putative ultradian rhythms that seemed to be emergent in *Six3-Cre;Lhx1*$^{lox/lox}$ mice. Based on this first pass, we screened the vigilance states of each individual mouse of all genotypes for ultradian rhythms of 2-3 hour period using JTK-Cycle [S1].

For # bouts analysis, the following bins useful for assessing sleep fragmentation were analyzed: "4 sec" = all bouts of 4 sec in length only, "32 sec" = all bouts from 32-56 sec in length, and "60 sec" = all bouts of 60 sec – 2 min in length.

Lipopolysaccharide (LPS) Studies
LPS was re-suspended in 0.9% sterile saline at a stock concentration of 1 mg/mL, aliquoted, and stored at -80C in siliconized Eppendorfs. During entrainment to 12:12 LD, mice were preconditioned with a single IP injection of 100ml per 5g body weight of 10mg/mL working concentration LPS, diluted from stock 1:100 in saline and stored on ice in siliconized Eppendorfs prior to injection. After entrainment and at least two weeks of free-running in DD, mice received three daily pulses of LPS (same dosage as preconditioning). The first pulse was administered at ~CT8 (or for totally arrhythmic mutants, at an arbitrary time), with subsequent pulses given at the same solar time as the initial pulse. After at least another two weeks in DD, another single LPS injection was given at CT8, and the mouse's behavior was tracked for at least an additional week. Vehicle control saline injections were given to some animals after LPS, and others naive to LPS; phenotypes were indistinguishable, and these were pooled for analysis. Our genetic control group used for telemetry studies is composed of both *Vip*$^{+/+}$ and *Lhx1*$^{lox/lox}$ animals; these showed indistinguishable responses to LPS, and were also pooled for analysis. Separate cohorts were used for telemetry and wheel running studies. The only data points excluded from our period and rhythm number analyses were in cases where mice became died, or the telemetry probe failed mid-experiment. For period calculations, arrhythmic mice also (obviously) had to be excluded. No statistical outliers were excluded. Statistical analysis was conducted in Graphpad Prism (ANOVA) and Free Statistics Calculators (2x3 Fisher's exact test).

Per2::Luc Data Collection and Analysis
Brains were removed after CO2 asphyxiation and placed in ice cold HBSS supplemented with 25 units/ml penicillin, 25 mg/ml streptomycin (Life Technologies). Brains were sliced in 300mm coronal sections on a World Precision Instruments vibroslicer. SCN were dissected by hand and placed on cell culture membrane inserts (Millipore PICMORG50) in 35mm culture dishes containing DMEM with B-27 supplement (Life Technologies), 352.5 mg/ml NaHCO3, 10 mM HEPES (Life Technologies), 25 units/ml penicillin, 25 mg/ml streptomycin (Life Technologies), and 0.1 mM luciferin potassium salt (Biosynth). Dishes were sealed with sterile vacuum grease and placed in a Lumicycle PMT (photomultiplier tube) apparatus (Actimetrics, Wilmette, IL) that was maintained in a 36^{o}C incubator. Tissues were heated for a duration of 3 hours per pulse to 38.5^{o}C at the indicated times by removal from the Lumicycle and placement on a heat block which was maintained in another 36^{o}C incubator. Tissues were transferred in light-tight pre-warmed insulated boxes. Phase changes were measured as in Buhr, et al. 2010. Briefly, the phase change was measured as the difference between the phase of Per2::Luciferase bioluminescence 3 days prior to the temperature pulse and 3 days after. Phases were measured by fitting a best-fit sine wave to at least 3 days of luminescence using the Lumicycle Analysis software.

Drugs: Tetrodotoxin purchased from Sigma, dissolved in water.

SCN Collection for RNA Sequencing
Brains were collected from *Six3-Cre;Lhx1*$^{lox/lox}$ and *Lhx1*$^{lox/lox}$ mice, or *Vip*$^{-/-}$ and *Vip*$^{+/+}$ mice between ~ZT6-9 on our animal facility's standard 15:9 light cycle, and placed ventral side up in a stainless steel brain matrix (Kent Scientific) pre-chilled on ice. Under a Leica MZ95 dissecting microscope, optic nerves were cut away and razor blades were positioned anterior and posterior to the SCN, using the optic chiasm as a landmark. Razors were pressed through the brain in one swift, smooth motion and brain surfaces anterior and posterior to the cuts were removed and examined, to ensure that the entire SCN was

captured. The razors were then removed and slowly hinged apart, using forceps to manipulate the slice fully onto one razor when necessary. Optic chiasm was gently removed from the resulting 1 mm thick brain slice with Bioscissors (Oban Precision Instruments) and forceps. SCN samples were taken using a 1 mm diameter stainless steel sample corer (Fine Science Tools) and deposited with forceps directly into Qiazol chilled on ice. Five SCN punches were pooled for each of three biological replicates per genotype.

After each biological replicate was dissected, tissues were homogenized in Qiazol using a Kimble Kontes motorized pellet pestle, and RNA was extracted using an RNeasy lipid tissue mini kit (Qiagen). RNA integrity was validated by Nanodrop (Thermo Scientific) and electrophoresis. A cDNA library was generated using a TruSeq Stranded Total RNA kit (Illumina). Libraries were barcoded and multiplexed 3 per lane, and sequenced to a paired-end read depth of 100 cycles on an Illumina HiSeq 2500. Fastq files were aligned using TopHat and fold changes were calculated using Cufflinks, both on Galaxy [S2,S3]. Shortlists of genes for closer examination were assembled by selecting transcripts meeting at least one of two primary criteria, and our secondary criterion. Tertiary analysis of this winnowed list was the final arbiter of *bona fide* hits. This analysis pipeline was executed separately for *Six3-Cre;Lhx1*$^{lox/lox}$ vs *Lhx1*$^{lox/lox}$ and *Vip*$^{-/-}$ vs *Vip*$^{+/+}$ comparisons. Our list of complete RNA-Seq hits was then subjected to pathway analysis using DAVID and Panther [S4–S6], as well as a manual literature search.
Primary Criterion 1: q-value<0.05
Primary Criterion 2: >2X average fold change and average control FPKM>1
Secondary Criterion: all individual cohorts show FPKM fold change consistent with average FPKM fold change
Tertiary Criterion: manual visual inspection of normalized peaks in all individual cohorts in the UCSC browser shows loss of expression consistent with average FPKM fold change.

A subset of transcripts clearly down in one or both of our mutants by ISH were missed by RNA-Seq. Many of these were likely due to contamination from adjoining anterior hypothalamic regions with substantial expression of these transcripts during dissection (e.g. *Avp*, *Penk*, *Ankfn1*), while others narrowly missed our primary or secondary criteria and were clearly down when examined visually post-hoc on the UCSC browser (e.g. *Grpr*, *Kit*, *Rasa4*).

Our raw RNA-sequencing data is publically available on the Sequence Read Archive, Accession Number SRP067306.

Supplemental References

[S1] Hughes, M., Hogenesch, J., and Kornacker, K. (2010). JTK_CYCLE: An efficient nonparametric algorithm for detecting rhythmic components in genome-scale data sets. J. Biol. Rhythms *25*, 372–380.
[S2] Goecks, J., Nekrutenko, A., Taylor, J., and Team, G. (2010). Galaxy: a comprehensive approach for supporting accessible, reproducible, and transparent computational research in the life sciences. Genome Biology *11*, R86.
[S3] Trapnell, C., Roberts, A., Goff, L., Pertea, G., Kim, D., Kelley, D., Pimentel, H., Salzberg, S.L., Rinn, J.L., Pachter, L., et al. (2012). Differential gene and transcript expression analysis of RNA-seq experiments with TopHat and Cufflinks. Nat Protocols *7*, 562–78.
[S4] Huang, D., Sherman, B., and Lempicki, R. (2008). Systematic and integrative analysis of large gene lists using DAVID bioinformatics resources. Nat. Protocols *4*, 44–57.
[S5] Huang, D., Sherman, B., and Lempicki, R.. (2009). Bioinformatics enrichment tools: paths toward the comprehensive functional analysis of large gene lists. Nucleic Acids Research *37*, 1–13.
[S6] Thomas, P., Kejariwal, A., Guo, N., Mi, H., Campbell, M., Muruganujan, A., and Lazareva-Ulitski, B. (2006). Applications for protein sequence–function evolution data: mRNA/protein expression analysis and coding SNP scoring tools. Nucleic Acids Research *34*, W645–W650.